Functional-Specific Projections from V2 to V4 in Macaque Monkeys

Chen Fang (201631430012@mail.bnu.edu.cn)
Beijing Normal University https://orcid.org/0000-0003-2196-3562
Kun Yan
Beijing Normal University
Chen Liang
Beijing Normal University
Jiayu Wang
Beijing Normal University
Xingya Cai
Beijing Normal University
Rui Zhang
Beijing Normal University
Haidong D. Lu
Beijing Normal University

Research Article

Keywords: optical imaging, retrograde tracing, V4, V2, functional architecture

Posted Date: March 18th, 2021

DOI: https://doi.org/10.21203/rs.3.rs-325966/v1

Abstract

Previous studies have revealed modular projections from area V2 to area V4 in macaques. Specifically, V2 neurons in cytochrome oxidase (CO)-rich thin and CO-sparse pale stripes project to distinct regions in V4. However, how these modular projections relate to the functional subcompartments of V4 remains unclear. In this study, we injected retrograde fluorescent tracers into different functional domains (color, orientation, and direction) in V4 that were identified with intrinsic signal optical imaging. We examined the labeled neurons in area V2 and their locations with respect to the CO patterns. Covariation was observed between the functional properties of the V4 injection sites and the numbers of labeled neurons in particular CO stripes. This covariation indicates that the color domains in V4 mainly received inputs from V2 thin stripes, whereas V4 orientation domains received inputs from pale (major) and thick (minor) stripes. Although there are motion-sensitive domains in both V2 and V4, our results did not reveal a functional-specific feedforward projection between them. These results confirmed previous findings of modular projections from V2 to V4 and provided functional specificity for these anatomical projections. Together, these findings indicate that color and form remain separate in the ventral midlevel visual processing.

Introduction

Area V2 in primates contains functionally distinct subcompartments that can be revealed with cytochrome oxidase (CO) staining. Thin CO stripes contain more color-sensitive neurons, thick and pale stripes contain more orientation neurons, and thick stripes contain more binocular disparity and direction neurons (DeYoe and Van Essen 1985; Hubel and Livingstone 1985, 1987; Peterhans and von der Heydt 1993; Levitt et al. 1994; Shipp and Zeki 2002). Functional imaging also confirmed such functional segregation in V2 (Ts'o et al. 1990, 2001; Roe and Ts'o 1995). These CO stripes also exhibit different patterns in projections to downstream areas. Neurons in thin and pale stripes mainly project to area V4, whereas neurons in thick stripes mainly project to area MT (DeYoe and Van Essen 1985; Shipp and Zeki 1985; Nascimento-Silva et al. 2003). In V2-V4 feedforward projections, thin and pale stripes appear to project to separate regions in V4 (Zeki and Shipp 1989; Nakamura et al. 1993; DeYoe et al. 1994; Felleman et al. 1997; Xiao et al. 1999), indicating a modular organization of V4 and modular connections with V2 functional organizations. However, the functional properties of these V2-receiving modules remain unclear. With the discovery of different types of functional modules in V4 (Ghose and Ts'o 1997; Conway et al. 2007; Tanigawa et al. 2010), it is important to establish the relationship between the anatomical and functional modules in V4.

Area V4 is an important visual area that performs midlevel visual processing (Roe et al. 2012; Pasupathy et al. 2020). Similar to its upstream areas, V4 also contains functional modules that preferentially process color and form information (Ghose and Ts'o 1997; Conway et al. 2007; Tanigawa et al. 2010). These spatially segregated modules may receive inputs from the corresponding color and form modules in V2. One of the purposes of this study was to provide direct evidence to support these functional connections between V2 and V4. Another potential functional connection we wanted to investigate was

motion-sensitive modules between these two areas. Previous studies have shown that in both V2 (Lu et al. 2010) and V4 (Li et al. 2013), direction-selective neurons tend to cluster and form functional modules. These findings inspired us to investigate the functional link between these two modules.

In this study, we first mapped 3 functional responses in V4 with intrinsic signal optical imaging. We then injected retrograde tracers into different V4 regions with different functional properties. Finally, we counted labeled neurons in different CO compartments in V2. We observed covariations between the labeled neurons in V2 and the functional properties of the tracer injection sites in V4; we then used this information to estimate the connections between V2 and V4 functional compartments.

Materials And Methods

Animal subjects

A total of 3 adult male macaque monkeys (2 *Macaca mulatta*, 1 *Macaca fascicularis*) were examined. All procedures were performed in accordance with the National Institutes of Health Guidelines and were approved by the Institutional Animal Care and Use Committee of Beijing Normal University.

Surgery

Aseptic surgery procedures were similar to those described in previous papers (Li et al. 2013). Animals were artificially ventilated and anesthetized with isoflurane (1.5-3%) in oxygen. Heart rate, end-tidal CO_2, blood oximetry, and body temperature were closely monitored, and anesthesia depth was estimated based on these values. A circular craniotomy (24 mm in diameter) was performed over area V4. The center of the craniotomy was 30-38 mm from the midline and 10-18 mm from the posterior bone ridge. A durotomy was performed to expose parts of areas V1, V2 and V4 (illustrated in Figure 1a&b).

Intrinsic signal optical imaging

Intrinsic signal optical imaging (ISOI) was performed immediately after surgery. The imaging procedures used were described in detail in previous papers (Li et al. 2013). The brain was stabilized with a cover glass (2-3 mm thickness) and agar (4%). The anesthetic was switched to propofol (induction 5 mg/kg, maintenance 5 mg/kg/hr, i.v.). To prevent eye movements, animals were paralyzed with vecuronium bromide (induction 0.25 mg/kg, maintenance 0.05 mg/kg/hr, i.v.) and respirated. Atropine sulfate (10 mg/ml) or tropicamide (5 mg/ml) was applied to dilate the pupils. Appropriate contact lenses were used to focus the eyes on a CRT screen 57 cm from the eyes. The cortex was illuminated with 632 nm light, and the reflectance light was collected by Imager 3001 (Optical Imaging Inc, Germantown, NY) at a 4 Hz frame rate. The frame size was 654´540 pixels, with a pixel size of 38 microns. Each imaging session started 0.5 seconds before the visual stimulus and lasted for 4 seconds (16 frames). The duration of the visual stimulation was 3.5 seconds. Intertrial interval was 8 seconds.

Visual stimulus

The visual stimuli used in this study were the same as those previously used to obtain functional maps (Lu et al. 2010 for V2 maps; Li et al. 2013 for V4 maps). Visual stimuli were created using ViSaGe (Cambridge Research Systems Ltd) and displayed on a 21-inch CRT monitor refreshing at 100 Hz. The stimulus patch was a square larger than 10 degrees, presented binocularly, and that fully covered the visual field of the imaged cortices. To obtain 3 types of functional maps (color, orientation, and direction), two sets of gratings were used. For the color functional map, responses to red-green isoluminant sinewave gratings and black-white sinewave gratings were compared. The spatial frequency (SF) of the gratings was 1 cycle/degree, and the temporal frequency (TF) of the gratings was 4 cycle/second. Gratings were presented in one of two orientations (45° or 135°) and in random directions orthogonal to the grating orientation. Data from different orientations were pooled. For orientation and direction maps, black-white square wave gratings were used. Gratings had an SF of 1 cycle/degree, had a TF of 4 cycles/second and drifted in one of 8 equally spaced directions (0°, 45°, 90°, 135°, 180°, 225°, 270°, or 315°). All stimuli were presented in a random order. An orientation map was obtained by comparing responses to orthogonal gratings (direction pooled), and a direction map was obtained by comparing responses to oppositely moving gratings.

Functional map guided tracer injection

V4 injection sites were selected from the 3 functional maps (color, orientation, and direction) with the aim of maximizing the response differences. Three types of tracers (CTB-488, CRB-555, and CTB-647) (1% Invitrogen) were used in this study. A pressure injection system (53311, Stoelting) and a glass pipette with a tip size of 23-35 mm (beveled) were used. The connection tube was filled with silicon oil, and the tracer was sucked into the glass pipette from its tip. A small amount of air (~40 nl) was sucked into the tip. The pipette was lowered to the planned V4 site based on the surface blood vessel pattern. The pipette tip was lowered into the cortex to a depth of 0.8-1.2 mm, and then was withdrawn 0.1 mm; next, the tracer injection was started. The amount of injection (30-100 nl, see Table 1) was measured starting at the air disappearing from the visible tip. After injection, the pipette was held in place for 10 min before retraction. The withdrawal distance of the pipette was recorded as the depth of the injection (see Table 1) when the tip left the cortex. One to 3 injections were given to each animal (different tracers for different functional sites). An imaging chamber (Li et al. 2013; Tang et al. 2020) was implanted. In vivo fluorescent images were examined (not shown) one week after the tracer injections to confirm tracer loading and to determine the center of the tracer diffusion.

Histology and areal delineation

Eighteen to 23 days after the tracer injections, the animals were sacrificed with an overdose of sodium pentobarbital (80-100 mg/kg) and perfused transcardially (step 1: 2 L of phosphate buffer, step 2: 1 L buffer with 2% paraformaldehyde, and step 3: 1 L buffer containing 2% paraformaldehyde and 10% sucrose; all pH 7.4). The brain tissue containing the lunate sulcus was separated, and the lunate was flattened. The tissue was postfixed in buffer containing 2% paraformaldehyde and 30% sucrose at room temperature for 2-3 h. Then, the tissue was cryoprotected in 30% sucrose buffer overnight at a

temperature of 4°C. The flattened tissue was sectioned horizontally on a freezing microtome (Rem-710, Yamato). Several hole markers were made with a used microelectrode perpendicular to the surface (with ~5 mm intervals) to aid subsequent alignments. The first slice, which contained surface blood vessels, was sectioned at a thickness of 120-150 mm, and the rest of the slices were 60-80 mm. Most of the slices were loaded onto a glass slide and sealed with cover glass for fluorescent imaging. For monkeys A, B and C, 3 (out of 11), 3 (out of 14), and 1 (out of 10) slices, respectively, were selected for CO staining (Wong-Riley 1979) and imaging (MVX10, Olympus, 1X objective).

For fluorescent imaging, we used a confocal microscope (A1R, Nikon) and a 10X objective. To determine the structure of labeled neurons, the software parameters (laser power, PMT amplification, offsets) were adjusted to make the labeled neuron sufficiently bright but not overexposed. For CTB-488, CTB-555, and CTB-647, we used 500-550 nm, 570-620 nm and 663-738 nm filters, respectively. These monochromatic images were colored green, red, and blue in software (Nis-Elements). These 3 images were then merged. In the merged images, neurons were identified manually based on their color: red, green, or blue neurons indicated CTB-488, CTB-555, or CTB-647, respectively; yellow, cyan, or magenta neurons indicated double-labeled neurons. We did not include triple-labeled neurons (white) since some non-neuronal noise (blood vessels and dust) also appeared white. These triple-labeled neurons accounted for less than 1% of the total labeled neurons. In the confocal images, the overexposure area around the injection site (due to the high density of labeled neurons) was determined as the size of the injection area (Table 1). Fluorescent label and CO staining images from adjacent slices were aligned according to the hole markers we made (imtransform, MATLAB). The ISOI maps and images of the first slice were aligned based on the surface blood vessel pattern. To determine the CO stripe, typically all the CO staining images of the same monkey were merged (monkeys A and B). CO stripes were identified based on the width of the densely stained stripes and their alternative patterns in a CO cycle. These slices were no longer suitable for fluorescent imaging. To obtain an accurate cell count, the labeled neuron numbers of these slices were estimated based on the averages of labeled neurons in their neighboring slices.

Data analysis

Functional maps

V4 functional maps (e.g., Figure 1d-f) were obtained with established SVM methods (Xiao et al. 2008; Chen et al. 2016). Compared with regular subtraction maps, SVM maps have a better signal/noise ratio while maintaining the linear relationship of the map signals. For each stimulus condition, we first obtained a dR/R image using the following formula: $dR/R = (R_{6\text{-}14} - R_{1\text{-}3})/R_{1\text{-}3}$, in which $R_{6\text{-}14}$ is the average of frames 6-14 and $R_{1\text{-}3}$ is the average of frames 1-3. Two sets of dR/R images (e.g., from color and luminance stimuli) were then used to train an SVM classifier (Libsvm, Chang and Lin 2011). An optimal classifier was obtained after 5-fold cross-validation. The weight map of the trained SVM classifier was used as the functional map (e.g., Figure 1d-f), in which a pixel value represents the contribution of the pixel to the classification. Each map was bandpass filtered (high cutoff: 0.1 mm/cycle, low cutoff: 3 mm/cycle).

Functional strength of the injection site

For area V4 in each case, we obtained 1 color map (color vs. luminance), 2 orientation maps (0° vs. 90° and 45° vs. 135°), and 4 direction maps (0° vs. 180°, 45° vs. 225°, 90° vs. 270°, and 135° vs. 315°). A color strength map was created with the absolute values of the color map pixels. Similarly, an orientation strength map created by taking the absolute values of the two orientation maps and combining them using the maximum value of each pixel. A direction strength map was obtained from the 4 direction maps with the same method. Each of the 3 functional strength maps was then filtered with a 1.5 mm-diameter circular mean filter and normalized to 0-1 (Figure 1g-i). The filtering procedure mimicked tracer diffusion (average diameter 1.5 mm). The pixel values of the 3 functional strength maps were then used as the functional strength values of the V4 injection sites in the following data analysis. In one case (monkey C), we also obtained 2 functional strength maps (orientation and direction) from area V2 and analyzed the spatial relationship between V2-labeled neurons and these strength maps (Figure 5g).

Correlation Analysis and linear regression

Spearman correlation (corr, MATLAB) was calculated between V4 functional strength values and numbers of V2-labeled neurons (Figure 3a-i), as well as between V4 functional strength values (Figure 4e-g). A linear regression (polyfit, MATLAB) was also calculated for each of these pairs. The goodness of fit was evaluated with R^2.

Results

A total of 3 hemispheres of 3 macaques were used in this study. For each hemisphere, color, orientation and motion direction maps were first obtained in anesthetized conditions with intrinsic optical imaging (Li et al. 2013). V4 regions with different functional properties were selected and used for tracer injection. For monkeys A and B, 3 injections of different tracers (CTB-488, 555, 647) were administered in one hemisphere for each animal. For monkey C, only one injection (CTB-647) was administered. Two to 3 weeks after injection, the animals were sacrificed. Area V2 was flattened, sliced and examined for labeled neurons under a confocal microscope. Some of these slices were stained and examined for CO compartments under a light microscope.

Functional properties of the V4 injection sites

Figure 1a-c shows the V4 injection sites in monkey A. This monkey had 3 injections, all of which were close to the foveal representation of V4. Figure 1d-f shows contrast maps obtained by comparing V4 responses to different visual stimuli. Black and white pixels in these maps represent regions preferentially activated by the stimuli illustrated on the left or right, respectively. Figure 1g-i shows the corresponding strength maps for the functional maps shown above. Each map was obtained by taking the maximal absolute values of a type of contrast map(s), normalizing and filtering (see Methods). Thus, the 3 injections targeted the color domain (blue cross), orientation domain (red cross), and direction domain (green cross). However, the 3 types of functional domains had some overlap. For example, the blue cross

was located in a color domain, which also had certain directional preferences. Each strength map (Figure 1g-i) was filtered with a circular mean filter whose diameter equaled the injection area, and the pixel value of the injection site (single pixel) was used as the functional strength for that injection site. Thus, for each injection, we obtained 3 functional strength values: color, orientation, and direction. The functional strength distributions were different for the 3 injections in monkey A (Figure 1j). Next, we examined whether such differences cause systematic changes in labeled neurons in V2.

Retrograde labeled neurons in V2

Eighteen to 23 days after the V4 injection, animals were sacrificed. Area V2 was flattened and cut into slices 60-80 mm thick. For each case, 1-3 slices were selected and used for CO staining to determine the CO stripe pattern in V2 (Figure 2b). Confocal fluorescent images were obtained from the rest of the slices (e.g., Figure 2c&d). Labeled neurons were manually identified from each slice and marked on a stripe-identified image (Figure 2e) after slice alignment. For each color (tracer), the labeled neurons formed several bands perpendicular to the V1/V2 border. In this case, CTB-488 (green)- and CTB-647 (blue)-labeled neurons were mostly located in thin stripes, whereas CTB-555 (red)-labeled neurons were mostly located in pale stripes (Figure 2e). Some labeled neurons were seen in thick stripes (mostly on their edges), but all 3 tracers were largely absent from thick stripes. In addition, we also observed that more superficial- and deep-layer neurons were labeled than those in the midlayers (not shown). For each tracer, we calculated the distribution of its labeled neurons among 3 stripe types (Figure 2f). To compare distributions among different tracers and cases, we used percentages of neurons instead of neuron numbers. CTB-647 (blue) was injected into a V4 region close to a color domain (Figure 1g), and its labeled neurons in V2 were mostly found in thin stripes (Figure 2f left). CTB-555 (red) was close to a V4 orientation domain (Figure 1h), and its V2 labeled neurons were mostly found in pale stripes (Figure 2f middle). For CTB-488 (green), the V4 injection site was close to a direction domain (Figure 1i), and its labeled neurons in V2 were mostly found in thin stripes (Figure 2f right). Thus, there appear to be certain correlations between the V4 injection site (and its functional properties) and the distribution of labeled neurons in V2. This qualitative observation is examined quantitively below. In total, we performed 7 injections in 3 hemispheres of 3 monkeys. Detailed information on the injection sites and labeled neurons in V2 is shown in Table 1.

V2-V4 correlation analysis

To analyze the relationship between the functional strengths of the V4 injections and the distributions of labeled neurons in V2 CO stripes, scatter plots of these two factors were used (Figure 3 a-i). Each plot comprises 7 data points, representing 7 tracer injections. For each injection, the X axis value represents its functional strength in one functional map, and the Y axis value represents its percentage of labeled V2 neurons in a certain stripe type. The dotted line is a linear regression of these data points.

Figure 3a shows that the percentages of labeled neurons in thin stripes were positively correlated with the color strength of the V4 injection sites. That is, when the injection site was closer to the center of the V4 color domains, more labeled neurons were found in the V2 thin stripes. Such a positive correlation was

not present in V2 pale ~ V4 color (Figure 3b) or V2 thick ~ V4 color (Figure 3c) plots. Taken together, these results indicated that V4 color modules tended to receive inputs from V2 thin stripes.

The V4 orientation feature had a positive correlation with V2 pale and thick stripes (Figure 3 e&f). The slope was steeper for pale stripes than for thick stripes, indicating a stronger contribution to V4 orientation domains from pale stripes than from thick stripes.

Figure 3g shows that the V4 direction had a positive correlation with V2 thin stripes. This is probably because many direction domains we selected for injection also had strong color responses (see Discussion). Figure 3h&i shows that the V4 direction had a negative correlation with both pale and thick stripes, indicating that the V4 direction domains did not tend to receive input from V2 pale or thick stripes. Since V2 direction neurons were more likely to be found in thick stripes, V4 direction domains are not likely to be a main efference for V2 motion. Further evidence from V2 imaging also supports this conclusion (Figure 5). For each plot, a Spearman correlation coefficient was calculated and illustrated in Figure 3j.

The slopes of the 9 plots in Figure 3a-i are not independent from each other. One reason is that the functional maps in V4 have certain spatial correlations. For example, the color and orientation domains in V4 tend to occupy complementary regions (Lu et al. 2010; Tanigawa et al. 2010). We analyzed functional maps in 12 V4 cases, including 3 cases in this study and 9 additional cases. The results confirmed previous findings and showed a negative relationship (Figure 4a). In addition, the selection of tracer injection sites is also important. In this case, the color and orientation properties of the 7 injection sites also showed a negative correlation (Figure 4e), consistent with the map features. In Figure 3, the slopes in the first and second rows are opposite to each other, which may reflect this negative relationship. In contrast, the V4 direction was positively correlated with V4 color (Figure 4b) and with V4 orientation (Figure 4c), consistent with previous findings (Li et al. 2013). Another factor that affects the independence of the scatter plot slopes is that V2 neuron numbers were normalized within a tracer group (to percentages). Thus, for 3 plots in a row, their slopes would not be the same sign (i.e., all positive or all negative). Normally, a weak positive slope or a zero slope may become negative because of this factor.

Thus, a positive correlation ($r > 0$) indicates that two factors were positively correlated. If two factors had no correlation ($r = 0$), the slope should be flat instead of negative. A negative correlation ($r < 0$) usually was due to some other factors (e.g., the negative correlation between V4 functional maps). Therefore, a positive correlation in Figure 3 was explained as the existence of a corresponding V2-V4 connection. A negative correlation was normally explained as an absence of a corresponding V2-V4 connection after taking into account multiple factors, including the spatial relationships between functional maps in V4 (Figure 4a-d), the properties of V4 injection sites (Figure 4e-h), and the normalization procedure for V2 neuron numbers.

In macaque monkeys, area V2 is mostly buried in the lunate sulcus, which limits the applicability of optical imaging. Thus, in this study, we mainly relied on CO staining to determine the V2 functional compartment. In monkey C, we also obtained functional maps of the V2 region containing labeled

neurons (Figure 5g) so that we could determine the functional properties of these V4-projecting neurons in addition to their CO properties. We only obtained V2 orientation and direction maps. This case only had one injection in V4, which had dual response features (color and direction) (Figure 4b&c). However, the labeled V2 neurons were mostly found in regions having weak direction and weak orientation responses (Figure 4 g, h, and i). Thus, this evidence confirmed earlier findings based on V2 CO stripes that V4 color and direction domains did not tend to receive inputs from V2 thick or pale stripes. This further suggests that the V4 direction domains do not receive direct input from the V2 direction domains.

Figure 6 summarizes our findings. In V2-V4 projection, V2 thin stripes mainly project to V4 color modules; V2 pale stripes mainly project to V4 orientation modules, and V2 thick stripes have much fewer projections to V4 than the other two stripes and mainly project to orientation modules. Pale and thick stripes do not project to V4 direction modules. It is not clear whether thin stripes project to V4 direction modules.

Discussion

In this study, we injected retrograde tracers into different functional modules in V4 and examined the patterns of labeled neurons in V2. We observed functional-specific projections from V2 CO stripes to V4 functional modules. In this study, functional and projection factors were quantified as was the correlation between these two factors. The results not only confirmed previous anatomical findings but also established a relationship between V2 CO stripes and V4 functional modules.

Parallel visual processing

The existence of functional modules, as well as the parallel projections among these modules, indicate that the process of visual information occurs in parallel. In V2-V4 projections, previous work has found that thin and pale stripes project to different regions in V4, whereas thick stripes barely project to V4 (DeYoe and Van Essen 1985; Zeki and Shipp 1989). The same projection patterns were also observed in New World monkeys (Nascimento-Silva et al. 2003, 2014). Our findings are generally in line with these earlier findings. The additional information we provide is the functional properties of these V4 targets. For orientation projection from V2 to V4, our data show that in addition to pale stripes, some thick neurons (mostly those located on the edges of thick stripes) also projected to V4 orientation domains. Our findings generally support the view that visual features are processed in parallel in the visual pathway.

However, much evidence has also shown that different visual features (color, form, motion, and depth) are not processed in parallel. A large degree of integration has been observed at both the single-cell and functional architecture levels. For example, many V2 neurons exhibit dual selectivity for color and orientation (Gegenfurtner et al. 1996; Shipp et al. 2009). Orientation and direction neurons are also found in thin stripes, and color neurons are found in pale and thick stripes (Gegenfurtner 2003). In general, it appears that parallel processing is more evident at the functional architecture level than at the single-cell level. This means that the same types of information (e.g., orientation) processed in different functional

modules (e.g., pale and thick stripes) is eventually sent to different downstream areas (e.g., V4 or MT). The functional significance of this processing strategy is worth further investigation.

Origin of V4 direction selectivity

Thus far, we have a relatively clear idea about the information sources for V4 color and orientation features. It is still unclear which inputs to V4 carry direction-selective motion information. It has been shown that many (~15%) V4 neurons have direction selectivity, some of which cluster into direction domains (Li et al. 2013). One potential region that provides input is V2, where direction neurons are mostly located in thick stripes. However, our results show that V4 direction domains do not receive inputs from V2 thick or pale stripes (Figure 3 h&i). In addition, our preliminary imaging results also show that V4 direction domains do not receive inputs from V2 direction domains (Figure 5 g&h). Thus, it appears unlikely that V4 direction domains obtained their motion inputs from V2 thick or pale stripes. For the positive correlation between the V4 direction and V2 thin stripes (Figure 3g), one possibility is that a major input to the V4 direction domain is V2 thin stripes, and V4 direction neurons indeed receive direction inputs from V2 thin projections. This possibility sounds less likely but not unreasonable, since there are direction neurons in V2 thin stripes, although they are fewer than those in thick stripes (Peterhans and von der Heydt 1993; Gegenfurtner et al. 1996). Another more likely possibility is that the phenomenon that V4 direction domains receive inputs from V2 thin stripes is an artifact. This is because the V4 injection sites we selected mostly had positively correlated color and direction strengths (Figure 4f), and it was V4 color neurons (not direction neurons) that received inputs from V2 thin stripe projections. In other words, we needed more differences in color and direction selectivity in our injection sites to differentiate their inputs. Compared with the V4 color domains, the clustering of the V4 direction domains was weaker (fewer neurons and less degree of clustering), and the tracing results were more likely dominated by the connection patterns of color neurons. If this is true (V4 direction domains do not receive inputs from V2 thin stripes), then V2 is unlikely the source of V4 direction selectivity.

Another potential source for V4 direction selectivity is area MT, since there are direct projections from MT to V4. However, a previous study selectively inhibited M or P layers in the LGN and found that V4 direction selectivity does not particularly rely on M or P input. This is different from what was observed in MT neurons, whose response mainly relied on M inputs (Maunsell et al. 1990; Ferrera et al. 1992, 1994). In this study, we also examined labeled neurons in MT, and the preliminary results indicated no correlation between V4 direction strength and labeled neuron numbers in MT (not shown). Thus far, there is no evidence showing that V4 direction neurons obtain direction selectivity from MT.

Since V4 receives inputs from many other visual areas (Ungerleider et al. 2008), all are potential sources for V4 direction selectivity. One study has shown that after V1 lesion, the response of V4 direction neurons is relatively better preserved than that of other types of V4 neurons (Schmid et al. 2013). This suggests that V4 direction-selective neurons may rely heavily on subcortical inputs that by-passing V1. In summary, V4 direction neurons do not seem to rely on inputs from V1, V2, or MT and form a spatialized group in V4 visual processing.

In addition to color, orientation, and direction, it has been shown that V4 has other functional architectures, such as size (Ghose and Ts'o 1997), curvature (Hu et al. 2020; Tang et al. 2020), and binocular disparity (Tanabe et al. 2005; Fang et al. 2019). The functional inputs from V2 for these V4 functional architectures can be studied in a similar way.

Declarations

Acknowledgments:

This work was supported by the National Natural Science Foundation of China (31625012, 31530029, and 31371111). We thank Dr. Xiaohui Zhang and Dr. Yousheng Shu for their valuable technical support. We thank lab members (Rendong Tang, Heng Ma, Qianling Song, Pengcheng Li, Jie Lu, Yan Xiao, Peichao Li, Jiaming Hu, Haoran Xu, Yang Fang) for their technical assistance.

Funding: National Natural Science Foundation of China (31625012, 31530029, 31371111).

Conflicts of interest/Competing interests: The authors declare no conflicts of interest.

Availability of data and material: Original data are available upon reasonable request

Code availability: Code are available upon reasonable request

Author Contributions: C.F., K.Y., C.L., J.W., R.Z. and X.C. performed the experiments; C.F., H.D.L. and K.Y. designed the research; C.F. performed the analysis; C.F. and H.D.L. interpreted the results and wrote the paper.

Ethics approval: All procedures were performed in accordance with the National Institutes of Health Guidelines and were approved by the Institutional Animal Care and Use Committee of Beijing Normal University.

Consent to participate: Not applicable.

Consent for publication: Consent for publication was obtained from all authors.

References

Chang C-C, Lin C-J (2011) LIBSVM: A library for support vector machines. ACM Trans Intell Syst Technol 2:1–27. https://doi.org/10.1145/1961189.1961199

Chen M, Li P, Zhu S et al (2016) An Orientation Map for Motion Boundaries in Macaque V2. Cereb Cortex 26:279–287. https://doi.org/10.1093/cercor/bhu235

Conway BR, Moeller S, Tsao DY (2007) Specialized Color Modules in Macaque Extrastriate Cortex. Neuron 56:560–573. https://doi.org/10.1016/j.neuron.2007.10.008

DeYoe EA, Felleman DJ, Van Essen DC, McClendon E (1994) Multiple processing streams in occipitotemporal visual cortex. Nature 371:151–154. https://doi.org/10.1038/371151a0

DeYoe EA, Van Essen DC (1985) Segregation of efferent connections and receptive field properties in visual area V2 of the macaque. Nature 317:58–61. https://doi.org/10.1038/317058a0

Fang Y, Chen M, Xu H et al (2019) An Orientation Map for Disparity-Defined Edges in Area V4. Cereb Cortex 29:666–679. https://doi.org/10.1093/cercor/bhx348

Felleman DJ, Xiao Y, McClendon E (1997) Modular Organization of Occipito-Temporal Pathways: Cortical Connections between Visual Area 4 and Visual Area 2 and Posterior Inferotemporal Ventral Area in Macaque Monkeys. J Neurosci 17:3185–3200. https://doi.org/10.1523/JNEUROSCI.17-09-03185.1997

Ferrera VP, Nealey TA, Maunsell JH (1992) Mixed parvocellular and magnocellular geniculate signals in visual area V4. Nature 358:756–758. https://doi.org/10.1038/358756a0

Ferrera VP, Nealey TA, Maunsell JH (1994) Responses in macaque visual area V4 following inactivation of the parvocellular and magnocellular LGN pathways. J Neurosci 14:2080–2088. https://doi.org/10.1523/JNEUROSCI.14-04-02080.1994

Gegenfurtner KR (2003) Cortical mechanisms of colour vision. Nat Rev Neurosci 4:563–572. https://doi.org/10.1038/nrn1138

Gegenfurtner KR, Kiper DC, Fenstemaker SB (1996) Processing of color, form, and motion in macaque area V2. Vis Neurosci 13:161–172. https://doi.org/10.1017/s0952523800007203

Ghose GM, Ts'o DY (1997) Form Processing Modules in Primate Area V4. J Neurophysiol 77:2191–2196. https://doi.org/10.1152/jn.1997.77.4.2191

Hu JM, Song XM, Wang Q, Roe AW (2020) Curvature domains in V4 of macaque monkey. eLife 9:e57261. https://doi.org/10.7554/eLife.57261

Hubel DH, Livingstone MS (1987) Segregation of form, color, and stereopsis in primate area 18. J Neurosci 7:3378–3415. https://doi.org/10.1523/JNEUROSCI.07-11-03378.1987

Hubel DH, Livingstone MS (1985) Complex–unoriented cells in a subregion of primate area 18. Nature 315:325–327. https://doi.org/10.1038/315325a0

Levitt JB, Kiper DC, Movshon JA (1994) Receptive fields and functional architecture of macaque V2. J Neurophysiol 71:2517–2542. https://doi.org/10.1152/jn.1994.71.6.2517

Li P, Zhu S, Chen M et al (2013) A Motion Direction Preference Map in Monkey V4. Neuron 78:376–388. https://doi.org/10.1016/j.neuron.2013.02.024

Lu HD, Chen G, Tanigawa H, Roe AW (2010) A Motion Direction Map in Macaque V2. Neuron 68:1002–1013. https://doi.org/10.1016/j.neuron.2010.11.020

Maunsell JH, Nealey TA, DePriest DD (1990) Magnocellular and parvocellular contributions to responses in the middle temporal visual area (MT) of the macaque monkey. J Neurosci 10:3323–3334. https://doi.org/10.1523/JNEUROSCI.10-10-03323.1990

Nakamura H, Gattass R, Desimone R, Ungerleider LG (1993) The Modular Organization of Projections from Areas V1 and V2 to Areas V4 and TEO in Macaques. J Neurosci 12:3681–3691. https://doi.org/10.1523/JNEUROSCI.13-09-03681.1993

Nascimento-Silva S, Gattass R, Fiorani M Jr, Sousa APB (2003) Three streams of visual information processing in V2 of Cebus monkey. J Comp Neurol 466:104–118. https://doi.org/10.1002/cne.10878

Nascimento-Silva S, Pinõn C, Soares JGM, Gattass R (2014) Feedforward and feedback connections and their relation to the cytox modules of V2 in *Cebus* monkeys. J Comp Neurol 522:3091–3105. https://doi.org/10.1002/cne.23571

Pasupathy A, Popovkina DV, Kim T (2020) Visual Functions of Primate Area V4. Annu Rev Vis Sci 6:363–385. https://doi.org/10.1146/annurev-vision-030320-041306

Peterhans E, von der Heydt R (1993) Functional Organization of Area V2 in the Alert Macaque. Eur J Neurosci 5:509–524. https://doi.org/10.1111/j.1460-9568.1993.tb00517.x

Roe AW, Chelazzi L, Connor CE et al (2012) Toward a Unified Theory of Visual Area V4. Neuron 74:12–29. https://doi.org/10.1016/j.neuron.2012.03.011

Roe AW, Ts'o DY (1995) Visual topography in primate V2: multiple representation across functional stripes. J Neurosci 15:3689–3715. https://doi.org/10.1523/JNEUROSCI.15-05-03689.1995

Schmid MC, Schmiedt JT, Peters AJ et al (2013) Motion-Sensitive Responses in Visual Area V4 in the Absence of Primary Visual Cortex. J Neurosci 33:18740–18745. https://doi.org/10.1523/JNEUROSCI.3923-13.2013

Shipp S, Adams DL, Moutoussis K, Zeki S (2009) Feature Binding in the Feedback Layers of Area V2. Cereb Cortex 19:2230–2239. https://doi.org/10.1093/cercor/bhn243

Shipp S, Zeki S (1985) Segregation of pathways leading from area V2 to areas V4 and V5 of macaque moneky visual cortex. Nature 315:322–324. https://doi.org/10.1038/315322a0

Shipp S, Zeki S (2002) The functional organization of area V2, I: Specialization across stripes and layers. Vis Neurosci 19:187–210. https://doi.org/10.1017/S0952523802191164

Tanabe S, Doi T, Umeda K, Fujita I (2005) Disparity-Tuning Characteristics of Neuronal Responses to Dynamic Random-Dot Stereograms in Macaque Visual Area V4. J Neurophysiol 94:2683–2699. https://doi.org/10.1152/jn.00319.2005

Tang R, Song Q, Li Y et al (2020) Curvature-processing domains in primate V4. eLife 9:e57502. https://doi.org/10.7554/eLife.57502

Tanigawa H, Lu HD, Roe AW (2010) Functional organization for color and orientation in macaque V4. Nat Neurosci 13:1542–1548. https://doi.org/10.1038/nn.2676

Ts'o DY, Frostig RD, Lieke EE, Grinvald A (1990) Functional Organization of Primate Visual Cortex Revealed by High Resolution Optical Imaging. Science 249:417–420

Ts'o DY, Roe AW, Gilbert CD (2001) A hierarchy of the functional organization for color, form and disparity in primate visual area V2. Vision Res 41:1333–1349. https://doi.org/10.1016/S0042-6989(01)00076-1

Ungerleider LG, Galkin TW, Desimone R, Gattass R (2008) Cortical Connections of Area V4 in the Macaque. Cereb Cortex 18:477–499. https://doi.org/10.1093/cercor/bhm061

Wong-Riley M (1979) Changes in the visual system of monocularly sutured or enucleated cats demonstrable with cytochrome oxidase histochemistry. Brain research 171:11–28. https://doi.org/10.1016/0006-8993(79)90728-5

Xiao Y, Rao R, Cecchi G, Kaplan E (2008) Improved mapping of information distribution across the cortical surface with the support vector machine. Neural Netw 21:341–348. https://doi.org/10.1016/j.neunet.2007.12.022

Xiao Y, Zych A, Felleman DJ (1999) Segregation and Convergence of Functionally Defined V2 Thin Stripe and Interstripe Compartment Projections to Area V4 of Macaques. Cereb Cortex 9:792–804. https://doi.org/10.1093/cercor/9.8.792

Zeki S, Shipp S (1989) Modular Connections between Areas V2 and V4 of Macaque Monkey Visual Cortex. Eur J Neurosci 1:494–506. https://doi.org/10.1111/j.1460-9568.1989.tb00356.x

Tables

Table 1. Case information

Case information		V4 injection information							V2 information				
Site	Animal	Tracer	Depth (mm)	Volumn (nl)	Area (mm^2)	Functional strength			Neuron number				CO
						Color	Orientation	Direction	Thin	Pale	Thick	Total	
No. 01	A	Ctb-488	1.60	30	1.24	0.36	0.15	0.96	9330	4565	1138	15033	++
No. 02	A	Ctb-555	1.30	30	1.45	0.11	0.50	0.28	593	3637	998	5228	++
No. 03	A	Ctb-647	1.40	30	1.76	0.96	0.16	0.77	3744	705	1080	5529	++
No. 04	B	Ctb-488	1.10	30	1.80	0.07	0.71	0.50	915	6242	4311	11468	++
No. 05	B	Ctb-555	1.30	30	2.10	0.76	0.33	0.76	3748	2142	736	6626	++
No. 06	B	Ctb-647	1.10	30	1.71	0.18	0.58	0.38	745	1793	392	2930	++
No. 07	C	Ctb-647	0.65	100	2.53	0.72	0.12	0.87	8839	3135	246	12220	+

++, good staining; +, normal;

Figures

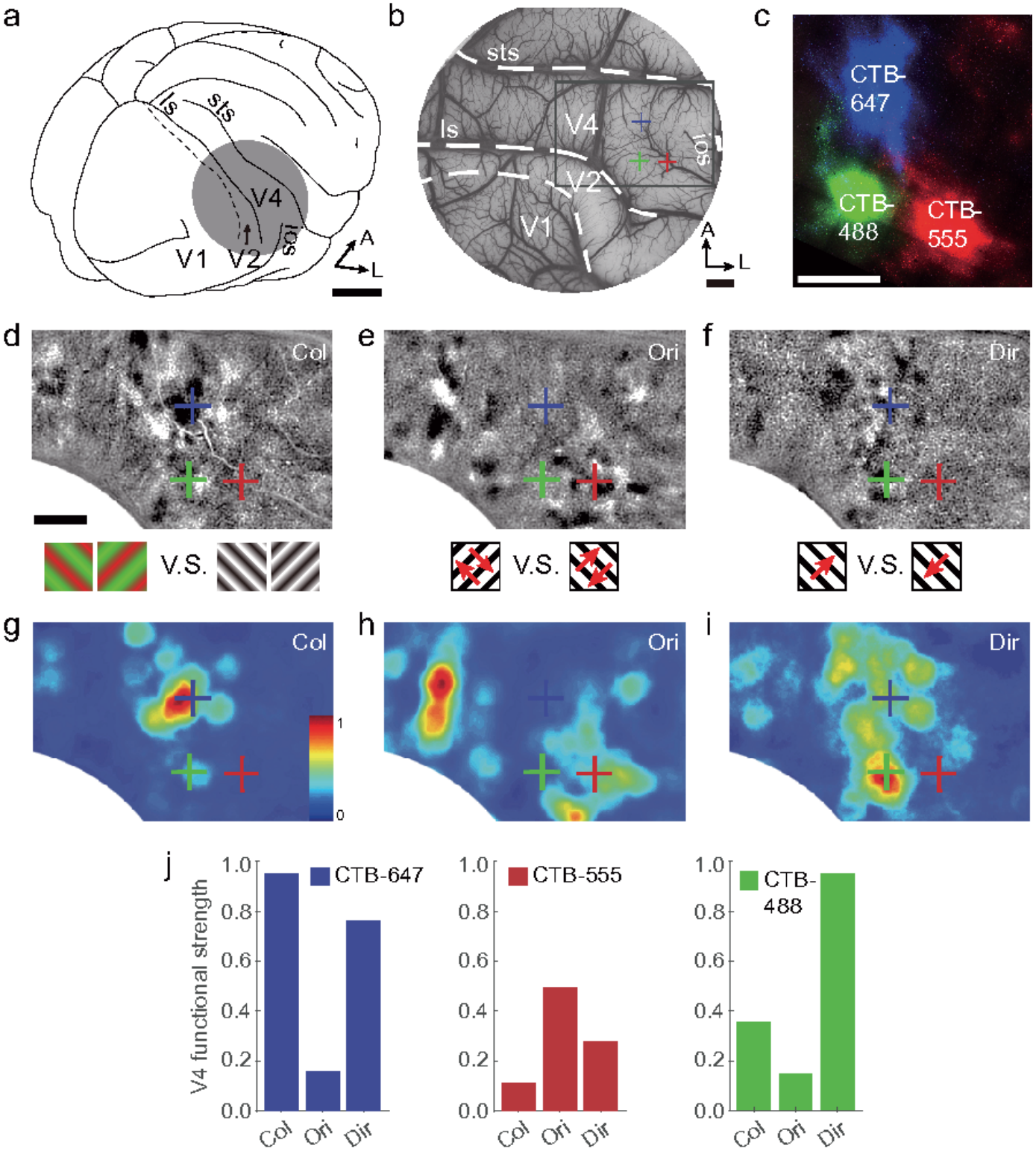

Figure 1

V4 functional imaging and tracer injection sites in monkey A a. An illustration of a macaque brain and the imaging chamber location. ls, lunate sulcus; sts, superior temporal sulcus; ios, inferior occipital sulcus. Scale bar: 10 mm. b. Surface blood vessel pattern of the imaging chamber in monkey A. Colored crosses mark the tracer injection site in V4 (green: CTB-488; red: CTB-555; blue: CTB-647). The black framed region is enlarged in d-i. Dashed lines represent area borders. Scale bar: 2 mm. c. Confocal fluorescent

image of a V4 slice showing the 3 injections. Scale bar: 2 mm. d. Color versus luminance map of area V4 (black framed region in b) obtained by comparing cortical responses to color and luminance gratings (illustrated below). The map was clipped at median ± 2.5 SD. Scale bar: 2 mm. e. An orientation-preference map for the same region. f. A direction-preference map for the same region. g-i: Functional strength map for color (g), orientation (h) and direction (i) obtained based on the contrast maps shown above. j: Normalized functional strength values for 3 injection sites, each with 3 values, corresponding to 3 functional maps.

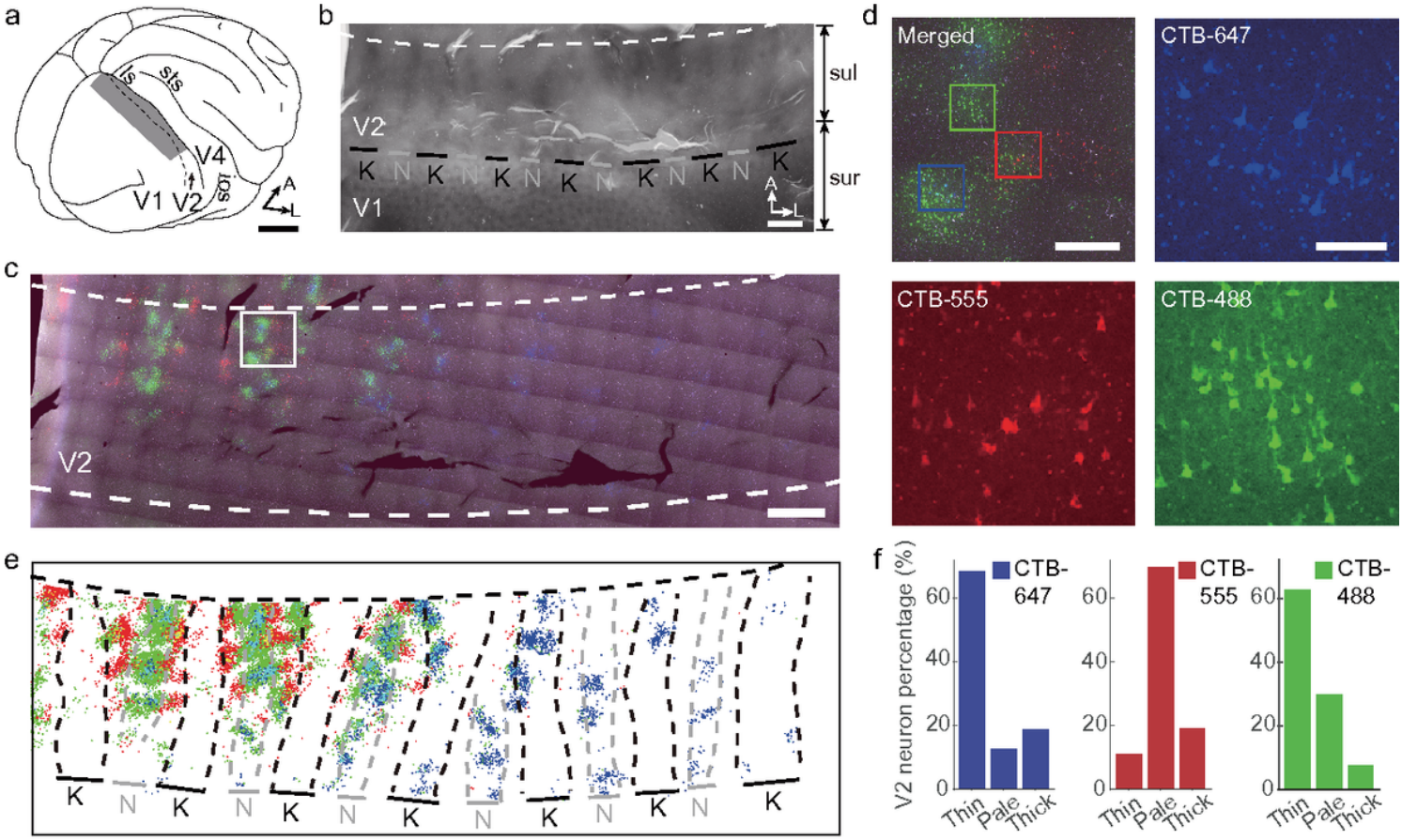

Figure 2

Retrogradely labeled neurons in V2 CO stripes in monkey A a. Illustration of macaque brain and regions of V2 (including V2 in the lunate sulcus) that were flattened. Scale bar: 10 mm. b. Average image of 3 slices stained with CO. Thin (N) and thick (K) stripes in V2 and blobs in V1. sul, area buried in sulcus; sur, area exposed on surface. Scale bar: 2 mm. c. A merged fluorescent image of a single V2 slice. Dashed lines are anterior and posterior borders of V2. The white framed region is magnified in d. Scale bar: 2 mm. d. Top left panel: a zoomed-in view of the framed region in c, scale bar: 0.5 mm. The other 3 panels are single-wavelength images of the corresponding framed regions of the same color in the top left panel (note that the color of these 3 images was added offline, not representing imaging light wavelengths). Scale bar: 0.1 mm. e. All labeled neurons overlaid on a CO stripe map after slice alignment. f.

Distributions of labeled neurons in 3 types of CO stripes for each tracer in monkey A. For comparisons among tracers, neuron numbers were normalized in each tracer and plotted as percentages.

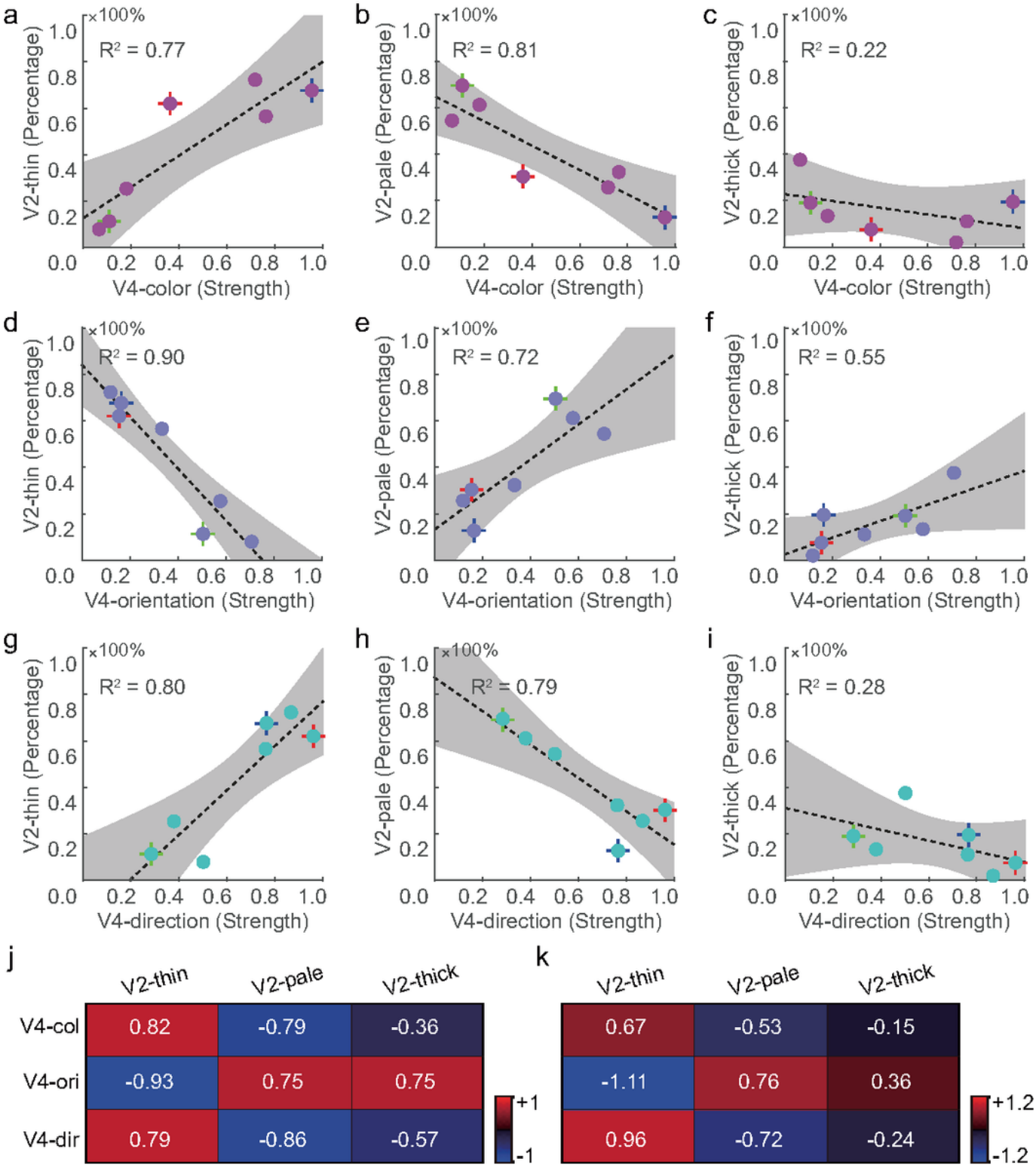

Figure 3

Correlation between V4 injection sites and V2-labeled neurons a-i. Scatter plot of injection site properties (X) and labeled neuron properties (Y) for all 7 injections (7 dots) in 3 monkeys. Dotted lines represent linear regression of the data points, and gray regions represent 95% confidence intervals. Dots with a

cross indicate data from the example cases shown in Figures 1 & 2 (Monkey A). j. Spearman correlation coefficients of the above 9 plots. k. Slope values of the line of fit in the above 9 plots.

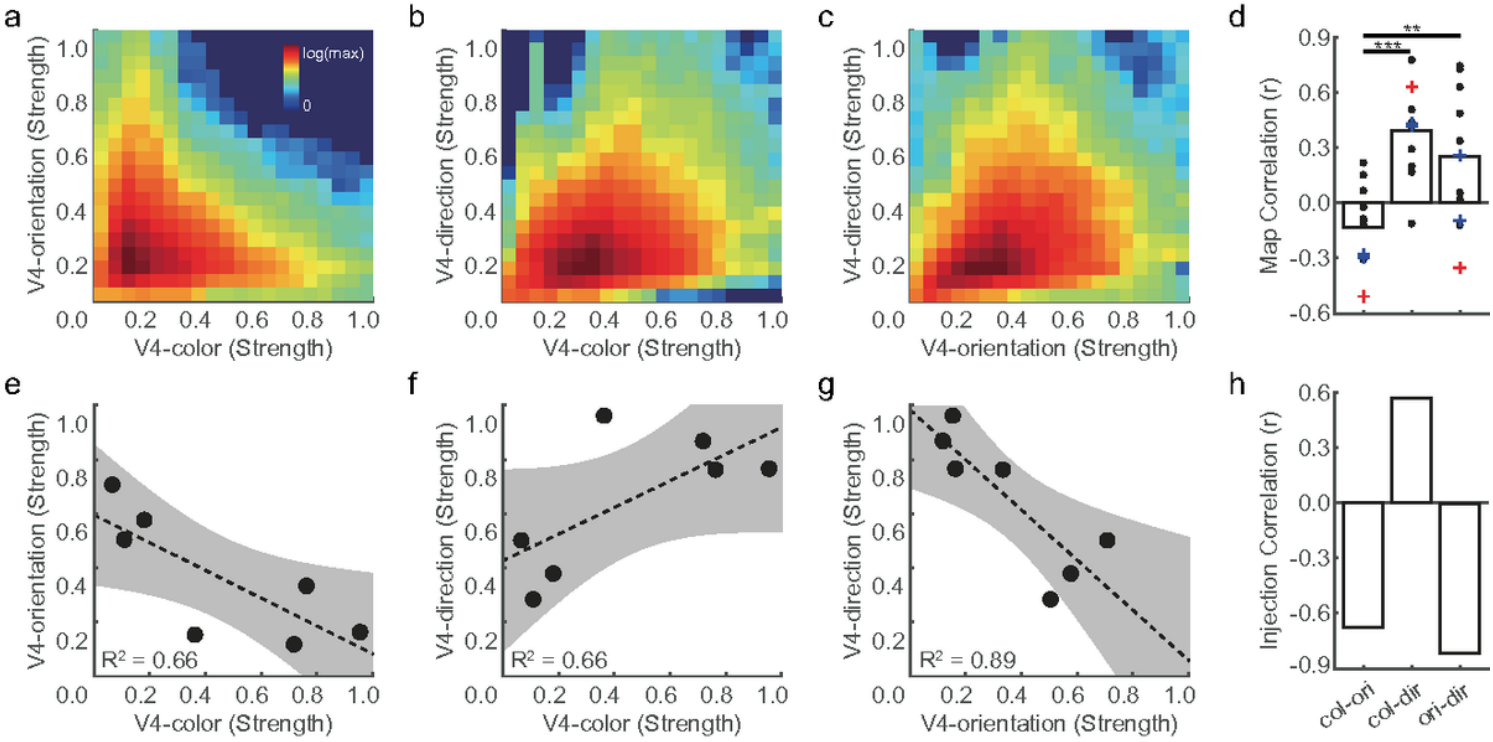

Figure 4

The V4 color and direction properties of the injection sites were covariant a. Pixel density map that shows pixel numbers (color) having certain color strength (X axis) and orientation strength (Y axis). This map shows the average of data from 12 cases. The color and orientation strengths were calculated in the same way as in Figure 1j. Strong color-selective pixels normally have weak orientation selectivity and vice versa. b. Similar to a but for direction and color strengths. Strong direction pixels tended to have strong color selectivity. c. Similar to a but for direction and orientation strengths. Strong direction pixels tended to have strong orientation selectivity. d. Correlation values for map pairs in a-c. Red crosses are from the example case shown in Figures 1 & 2 (monkey A), blue crosses are for monkeys B and C. **, t-test $p < 0.01$; ***, $p < 0.001$. e-g. Scatter plots of different injection site properties for all 7 injections (7 dots). h. Spearman correlation values for scatter plots in e-g.

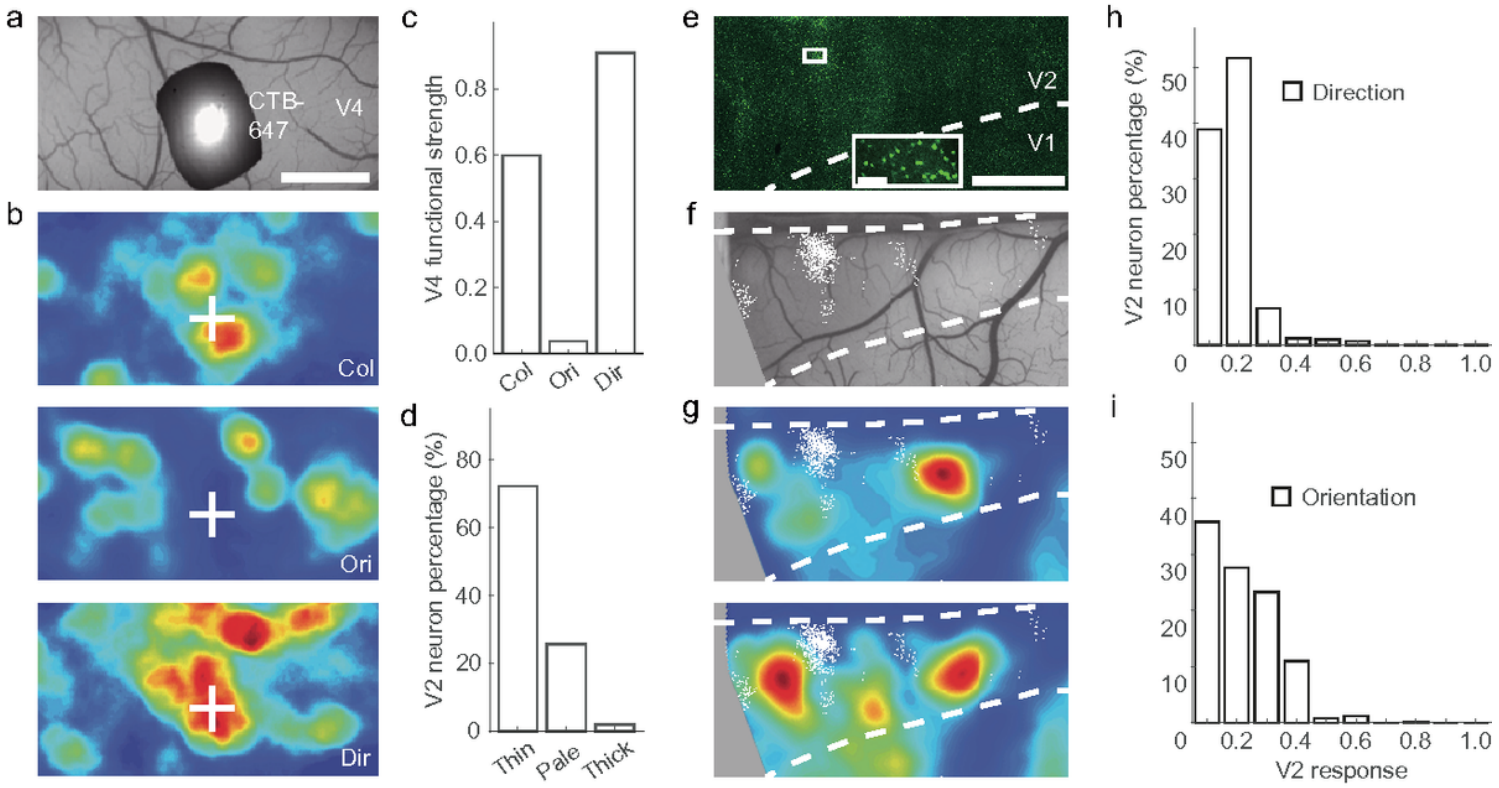

Figure 5

Functional properties of V4 injection sites and labeled V2 neurons in monkey C a. A single injection in V4 in monkey C. Scale bar: 2 mm applied to a-b. b. The location of the injection site in 3 functional maps. c. The functional strength of the V4 injection site. d. Normalized distribution of labeled neurons in 3 types of V2 stripes. e. A single fluorescent image of a V2 slice; green color was added for better viewing. Scale bar: 2 mm, applies to e-g. Insert: a zoomed-in view of the framed region, scale bar: 0.1 mm. f. In vivo blood vessel map of area V2 superimposed with labeled neurons (white dots). g. Functional maps for orientation (top) and direction (bottom). h. Distribution of orientation map strength at locations of the labeled neurons. i. Similar to h, but for the direction map.

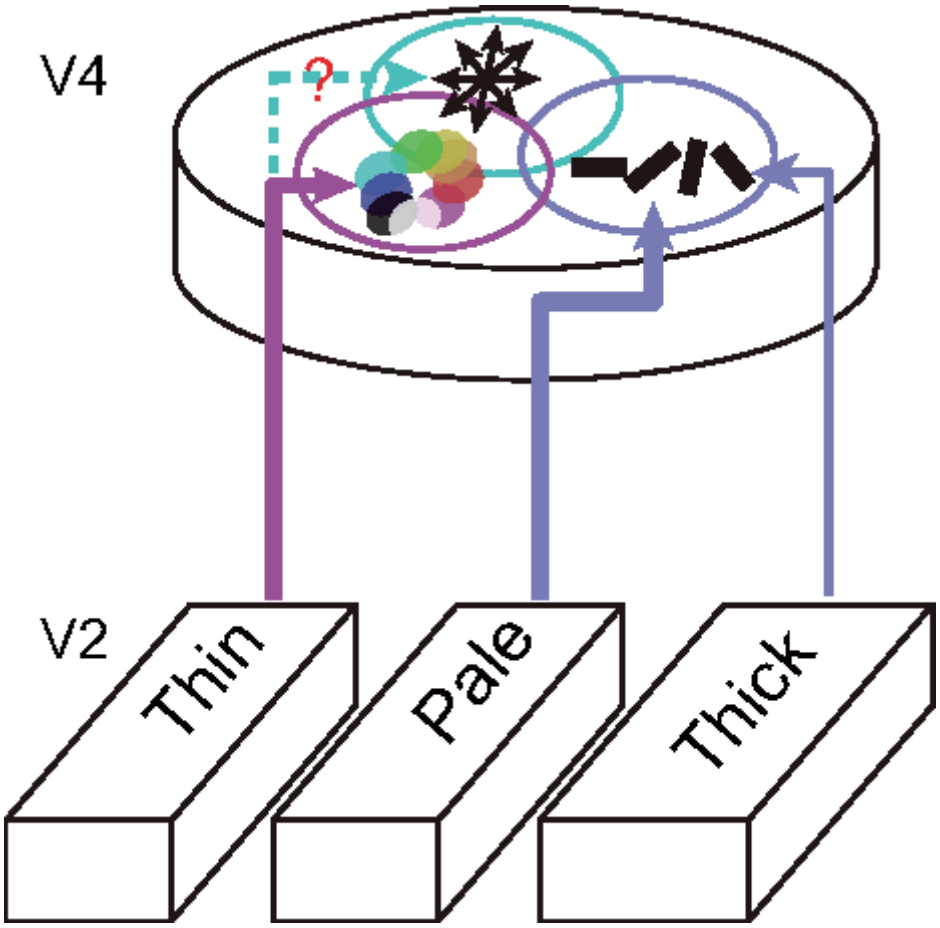

Figure 6

Summary of functional inputs to V4 from V2 A summary diagram showing the strength of projections from V2 to V4. In V2-V4 projections, V4 color domains mainly receive inputs from V2 thin stripes, whereas V4 orientation domains mainly receive inputs from V2 pale (major) and thick (minor) stripes. Though it is still unclear whether V4 direction domains receive inputs from V2 thin stripes, it is clear that they do not systematically receive inputs from thick or pale stripes.